Genomics Proteomics Bioinformatics 12 (2014) 19–30

Genomics Proteomics Bioinformatics

www.elsevier.com/locate/gpb
www.sciencedirect.com

ORIGINAL RESEARCH

Expression of miR-15/107 Family MicroRNAs in Human Tissues and Cultured Rat Brain Cells

Wang-Xia Wang [1], Robert J. Danaher [2], Craig S. Miller [2], Joseph R. Berger [3], Vega G. Nubia [3], Bernard S. Wilfred [1], Janna H. Neltner [1,5], Christopher M. Norris [4,5], Peter T. Nelson [1,5,*]

[1] *Sanders-Brown Center on Aging, University of Kentucky, Lexington, KY 40536, USA*
[2] *College of Dentistry, University of Kentucky, Lexington, KY 40536, USA*
[3] *Department of Neurology, University of Kentucky, Lexington, KY 40536, USA*
[4] *Department of Molecular and Biomedical Pharmacology, University of Kentucky, Lexington, KY 40536, USA*
[5] *Department of Pathology, University of Kentucky, Lexington, KY 40536, USA*

Received 16 May 2013; revised 9 September 2013; accepted 6 October 2013
Available online 28 January 2014

Handled by Andreas Keller

KEYWORDS

miR-16;
miR-424;
miR-503;
miR-15;
Normalization;
Target prediction

Abstract The miR-15/107 family comprises a group of 10 paralogous microRNAs (miRNAs), sharing a 5′ AGCAGC sequence. These miRNAs have overlapping targets. In order to characterize the expression of miR-15/107 family miRNAs, we employed customized TaqMan Low-Density micro-fluid PCR-array to investigate the expression of miR-15/107 family members, and other selected miRNAs, in 11 human tissues obtained at autopsy including the cerebral cortex, frontal cortex, primary visual cortex, thalamus, heart, lung, liver, kidney, spleen, stomach and skeletal muscle. miR-103, miR-195 and miR-497 were expressed at similar levels across various tissues, whereas miR-107 is enriched in brain samples. We also examined the expression patterns of evolutionarily conserved miR-15/107 miRNAs in three distinct primary rat brain cell preparations (enriched for cortical neurons, astrocytes and microglia, respectively). In primary cultures of rat brain cells, several members of the miR-15/107 family are enriched in neurons compared to other cell types in the central nervous system (CNS). In addition to mature miRNAs, we also examined the expression of

* Corresponding author.
E-mail: pnels2@email.uky.edu (Nelson PT).

Peer review under responsibility of Beijing Institute of Genomics, Chinese Academy of Sciences and Genetics Society of China.

http://dx.doi.org/10.1016/j.gpb.2013.10.003

precursors (pri-miRNAs). Our data suggested a generally poor correlation between the expression of mature miRNAs and their precursors. In summary, we provide a detailed study of the tissue and cell type-specific expression profile of this highly expressed and phylogenetically conserved family of miRNA genes.

Introduction

MicroRNAs (miRNAs) are short non-coding RNAs that are expressed in all known plant and animal cells. MiRNAs are estimated to regulate the translation of well over half the transcripts in the human genome [1–3]. Derived from a larger RNA precursor (pri-miRNA), the miRNA transcript is processed in a multistage sequence, culminating in the cleavage of a short hairpin RNA to form a mature ~22 nucleotide miRNA [4]. In animal species, miRNAs regulate gene expression at the post-transcriptional level, via imperfect sequence complementarity with "target" mRNA, which results in either mRNA translational suppression or degradation [5]. An essential regulatory portion of mature miRNA is the 'seed' region near the 5′ end of a miRNA [1,6].

The focus of the current study is a group of paralogous, evolutionarily-conserved miRNAs termed the miR-15/107 family [7–9]. This group of miRNAs shares a sequence (AGCAGC) near the 5′ end [7] that complements with an overlapping list of mRNA targets [10,11]. Members of the miR-15/107 family play key roles in gene regulation involved in cell division, metabolism, stress response and angiogenesis [7]. The miR-15/107 group has been implicated in pathological processes including cancers, cardiovascular disease and neurodegenerative diseases. While all vertebrates examined to date express miR-15a, miR-15b, miR-16, miR-103 and miR-107, only mammals are known to express miR-195, miR-424, miR-497, miR-503, whereas miR-646 appears to be human-specific [7].

Among the key characteristics of any miRNA are the types of tissues and cells where a specific miRNA is expressed. Thus, miRNA expression profiling is an essential tool for understanding which genes are transcribed (pri-miRNAs) and processed to mature miRNAs in various organs and cells. Although there have been prior expression profiling studies of miRNAs in human tissues (see below), the particular expression profiles of all miR-15/107 family genes have not been thoroughly described either in human tissues or in terms of the specific cell types of the central nervous system (CNS). To address this, we examined and here report on the expression of miR-15/107 miRNAs in both human tissues and in individual cell types of the cultured rat brain cell preparations. This study also presents data using a relatively novel RT-qPCR-based method for miRNA quantitation.

Results

miR-15/107 family miRNAs are highly expressed in human brain with overlapping targets

Mature miRNAs of miR-15/107 family share a sequence (AGCAGC) near the 5′ end (**Figure 1A**), and multiple family members are expressed at high levels in the human brain tissue (**Figure 1B**). Analysis of RNA deep sequencing data generated from human brains [12] revealed that miR-15/107 family accounts for 1.5–2.0% of total miRNA reads in the temporal neocortex (Brodmann areas 21/22) gray matter of non-demented control brains. From RNA isolated from these human brain samples, miR-16, miR-103, miR-107 and miR-497 are the most highly expressed miRNAs among the family members. Biochemical identification of miR-16, miR-103, miR-107 and miR-497 targets in H4 glioneuronal cell line showed that these miRNAs share high degrees of overlap in targets (**Figure 1C**) with 20% of mRNA targets shared by all 4 miRNAs.

Multiple mature miRNAs of miR-15/107 family members show robust expression in different human tissues

A custom designed PCR-array panel was used, including 10 miR-15/107 members and the other 10 selected miRNAs (Table S1) to profile the miRNA expression from 11 human tissues. Demographic information on the human autopsied cases is provided in Table S2. Relatively high levels of miRNA expression were observed across different human tissues with PCR Ct values ranging from 15 (miR-16) to 35 (miR-646) (**Figure 2**) in some tissue samples. Hierarchical clustering (Pearson's correlation-Average Linkage) based on the similarity of miRNA expression patterns of the 11 tissues demonstrated that similar anatomical tissues were generally clustered together. For example, cerebral cortex, frontal cortex and primary visual cortex showed similar miRNA expression pattern, resulting in close clustering; similarly, heart and skeletal muscle samples demonstrated similar expression patterns. The heat map also showed a clustering of miRNA expression pattern for a given tissue type (between cases), indicating an organ-specific expression pattern. For detailed quantitative data, see Tables S3 and S4.

Further analysis revealed a distinct expression profile of brain-enriched miRNAs (**Table 1** and **Figure 3**). For example, miR-124a, a known brain-enriched miRNA, was strongly expressed in brain tissues as expected with lower levels of expression in the kidney, spleen and skeleton muscle samples (expression marked as "undetectable" when Ct > 35). miR-107 was also shown to be enriched in brain tissues (3.25-fold, $P < 0.0001$). Similarly miR-103 and Let-7a tended to be expressed at higher levels in brain tissues, whereas miR-16, miR-15a, miR-15b, miR-424, miR-497, miR-503, miR-646 and other non-miR-15/107 miRNAs (miR-20a, miR-23a, miR-27a, miR-27b, miR-30d, miR-143) tended to show higher expression in non-brain tissues (Figure 3 and Table 1). Comparison of miRNA expression among individual tissue types showed that miR-15a, miR-15b and miR-16 were enriched in the spleen, miR-424 was expressed relatively high in the kidney, liver and skeletal muscle, and miR-646 was enriched in the kidney.

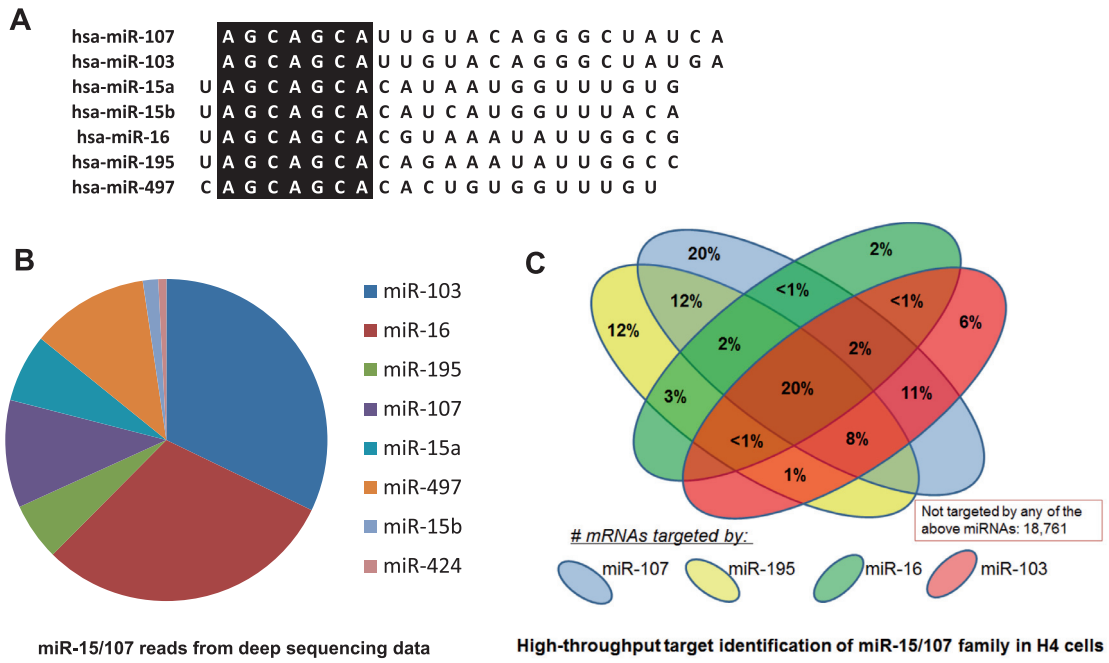

Figure 1 Highly expressed miR-15/107 miRNAs with overlapping targets
A. Members of miR-15/107 share a homologous 5′ sequence. Shown here are the miR-15/107 miRNAs that are highly expressed in human tissues. **B.** Normalized miRNA reads for miR-15/107 family from deep sequencing RNA-seq data. RNA was prepared from two cognitively intact persons' temporal lobe brain samples [12]. **C.** Biochemical identification of miR-16, miR-103, miR-107 and miR-497 targets according to methods previously published [49,50] revealed extensive but non-identical overlapping targets in H4 cells. This not only shows the importance of the 'seed' regions, but also indicates that non-seed portions of the miRNAs are important as well. In this assay, 18,761 mRNAs were not targeted by any of these miRNAs.

Members of the miR-15/107 family are enriched in neurons

The expression of miR-15/107 family miRNAs was evaluated in different brain cell types. Primary rat neuron, astrocyte and microglia cultures were obtained from rat pups at embryonic day 18 (E18) (see Materials and methods). The cell-type enriched cultures were verified by Western blot analysis using antibodies against cell-type specific markers (**Figure 4**).

The expression of all tested miRNAs was different between neuronal (cerebral cortical neurons) and non-neuronal (cerebral cortical astrocytes and microglial) cells (**Figures 5** and **6**, **Table 2**). In contrast, astrocytes and microglial share relatively similar expression profiles (Table 2). Specifically, 4 members of the miR-15/107 family (miR-103, miR-107, miR-195 and miR-497) were among the neuron-enriched miRNAs (> 2-fold enriched for each, $P < 0.05$). Other neuron-enriched miRNAs include miR-124, miR-20a, miR-320 and Let-7a miRNAs (Figures 5 and 6, Table 2), whereas miR-23a, miR-27a, miR-29a, miR-29b and miR-143 were glial-enriched (both $P < 0.05$).

Expression of pri-miRNAs is correlated relatively weakly with that of mature miRNAs in miR-15/107 family

Diverse expression profiles were found for miRNA precursors (pri-miRNA) in human tissues (**Figure 7** and Table S5). The expression of miR-124 precursor was exclusively identified in the brain tissues, which is well correlated with its neuronal expression characteristics. In contrast, miR-23a precursor was expressed at relatively high levels in non-brain tissues (**Table 3**).

Correlations between expression of the fully processed (~22 nt, *i.e.*, "mature") miRNA and precursor transcript expression were generally not strong for most miRNAs (**Table 4** and Figure S1). Among the 23 miRNAs tested, miR-124, a brain and neuron-specific non-miR-15/107 family miRNA, showed the strongest correlation ($R^2 = 0.9189$) between precursor and mature miRNA. The mature miR-103 can potentially be generated from two primary miRNA transcripts that are encoded from different chromosomes [13]. The array data showed that expression of mature miR-103 shows a tighter correlation with miR-103a-2 precursor (hsa-miR-103a-2-Hs03302758_pri, Table 4 and Figure S1), which was expressed at relatively high levels across all tested tissues. The expression levels of miR-103a-2 precursor were higher than that of miR-103a-1 (fold increase of 1.8–72.8, **Table 5**). These data indicate that mature miR-103 in humans appears to be mainly generated from miR-103a-2 precursor that resides in PANK2 gene.

We also examined the expression of some non-miR-15/107 miRNA genes. The human miR-29 family includes three mature members, miR-29a, miR-29b and miR-29c, that are encoded by two gene clusters. The gene encoding the precursors of both miR-29b-1 and miR-29a is located on Chromosome 7, whereas the coding gene for both miR-29b-2 and miR-29c is on Chromosome 1 [14]. Among the three

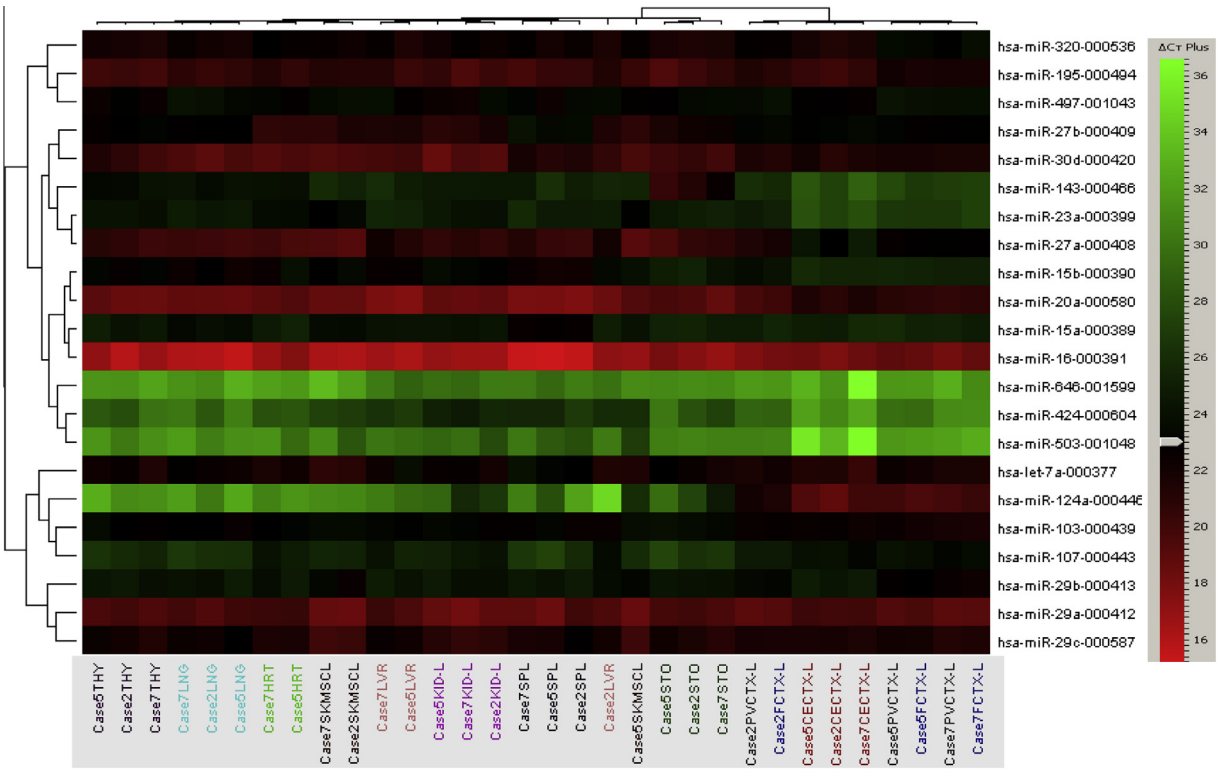

Figure 2 Hierarchical clustering of miRNA expression in human tissues

Ct values of each assay were normalized using the global mean method. The average linkage of the clustered group was calculated using the Pearson's correlation method. Tissues of the same or similar anatomic origin were clustered together, indicating discernible tissue-type specific expression patterns for these miRNAs. Each tissue groups were marked in the same colors. CECTX-L, cerebral cortex (left); FCTX-L, frontal cortex (left); PVCTX-L, primary visual cortex (left); THY, thymus; HRT, heart; LNG-L, lung (left); LVR, liver; KID-L, kidney (left); SPL, spleen; STO, stomach; SKMSCL, skeletal muscle.

Table 1 Relative expression of mature miRNAs in the human brain tissue

miRNA	Fold change	*P* value
hsa-let-7a	1.63	0.0233
hsa-miR-103	1.73	0.0003
hsa-miR-107	3.25	0.0000
hsa-miR-124a	978.04	0.0000
hsa-miR-143	0.120	0.0000
hsa-miR-15a	0.481	0.0001
hsa-miR-15b	0.272	0.0000
hsa-miR-16	0.295	0.0000
hsa-miR-195	0.588	0.021
hsa-miR-20a	0.222	0.0000
hsa-miR-23a	0.196	0.0008
hsa-miR-27a	0.165	0.0004
hsa-miR-27b	0.498	0.0003
hsa-miR-29a	0.935	0.6897
hsa-miR-29b	0.645	0.1147
hsa-miR-29c	0.962	0.7846
hsa-miR-30d	0.334	0.0000
hsa-miR-320	0.719	0.1871
hsa-miR-424	0.107	0.0001
hsa-miR-497	0.769	0.1212
hsa-miR-503	0.144	0.004
hsa-miR-646	0.375	0.0524

Note: Expression of miRNAs in the human brain tissue is normalized to that in non-brain tissues and presented as fold change. Expression that is significantly higher or lower in brain is highlighted in red and green, respectively ($P < 0.05$). Members of miR-15/107 family are highlighted in blue.

miR-29 precursor transcripts tested (due to limited number of gene spots on the array card, miR-29b-2 was not included), primary miR-29b-1 (hsa-miR-29b-1-Hs03302748_pri) seemed to be the major expresser in most tissues (Table S6). In contrast to much higher levels of mature miR-29a and miR-29c, expression of miR-29a precursor was not detected (Ct > 40) in the kidney, liver and spleen; likewise, expression of miR-29c was not detected in lung and spleen. This is interesting because miR-29a and miR-29b-1, like miR-29b-2 and miR-29c, are apparently co-transcribed as polycistronic primary transcripts [15].

Discussion

Here we report for the first time a systematic expression analysis of all miR-15/107 genes in various human tissues and in different rat CNS cell types. Individual members of the miR-15/107 group are expressed at medium-to-high levels across many tissue types but there is some tropism in terms of both tissue- and cell type-specific expression. While these data provide novel results about the expression of miR-15/107 genes, there is not, among these miRNAs, a sharply tissue- or cell-specific miR-15/107 gene. Since miR-15/107 miRNAs (like many other miRNAs that have co-evolved with paralogs) co-exist alongside highly-expressed miRNAs with overlapping targets [7,16], these data provide support to the idea that it is necessary to take into account the expression and activities

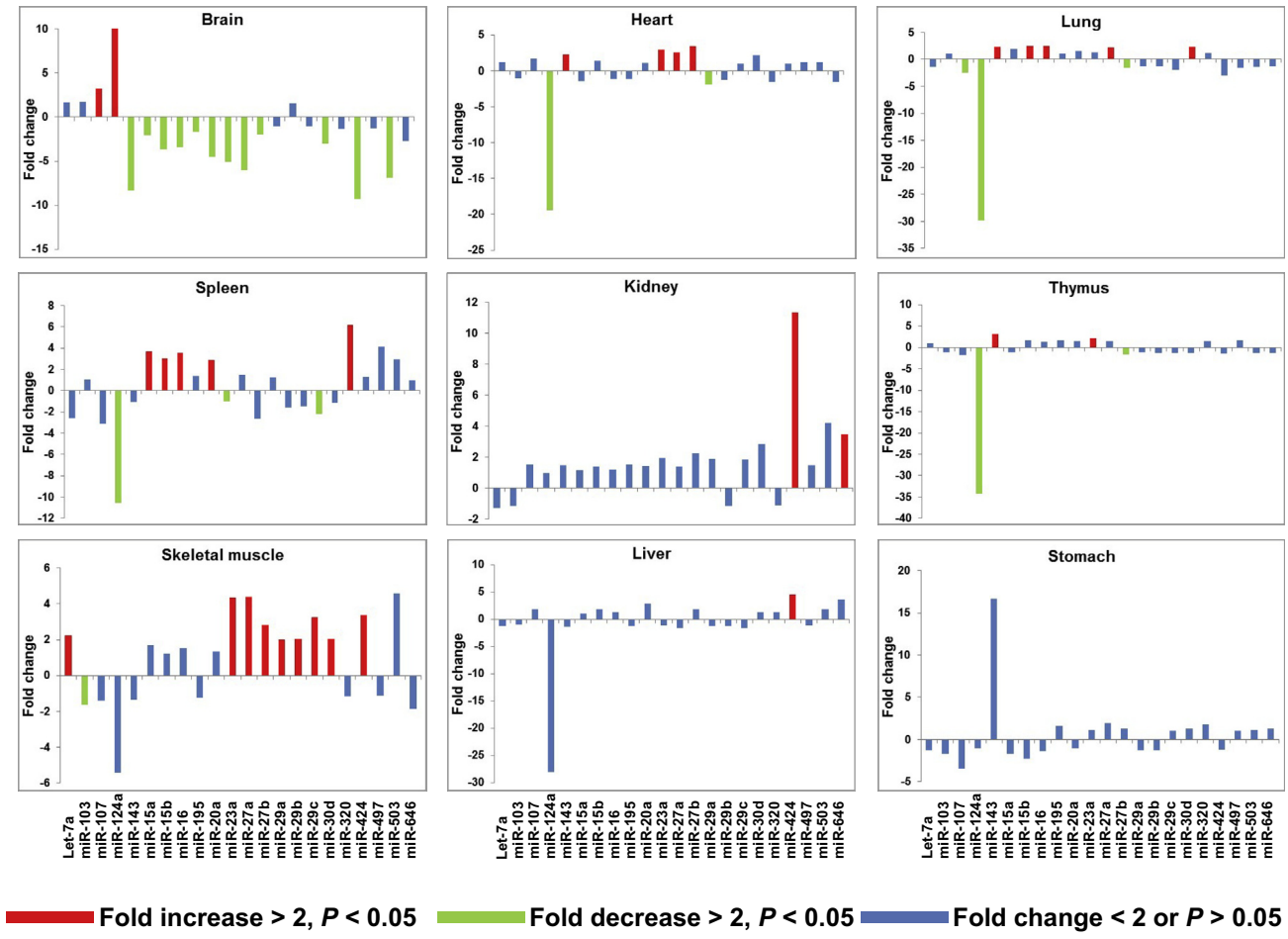

Figure 3 Expression profiles of miRNAs in different human tissues

Levels of miRNA expression in each individual tissue were calculated as fold difference against the other tissues examined. Bars in red indicated a significantly higher expression level (> 2-fold), and bars in green indicated a significantly ($P < 0.05$) lower expression level (> 2-fold) compared to the other tissues. Expression showing no statistical difference between a particular tissue type and the others was indicated in blue.

of paralogous miRNAs, rather than just focusing on individual miRNAs in isolation.

There are some technical caveats to our study. Much of the data derive from human subjects who came to autopsy. This experimental approach introduces potential biases such as those related to agonal events, comorbidities and ascertainment/recruitment bias. RNA from autopsy specimens can also be degraded. An alternative approach would have been to use surgical pathologic specimens from multiple different individuals. This approach would have introduced a separate but overlapping list of potential pitfalls such as epiphenomena linked to surgery (anesthesia-related RNA expression changes), additional inter-individual variability and strong ascertainment biases. For example, persons undergoing stomach surgery differ systematically from those undergoing liver surgery. Faced with the alternatives, using autopsy material is defensible, but the data should be analyzed with caution in light of these concerns. In addition to the pre-analytical potential challenges, researchers from many laboratories have now found that miRNA profiling results obtained using different platforms can vary dramatically for individual miRNAs despite good overall inter-platform correlation [17–21].

Keeping the technical challenges in mind, our data provide new insights into the expression of the miR-15/107 gene family in humans. A straightforward observation is that the miRNAs with highest expression in human tissues (miR-15a, miR-15b, miR-16, miR-103, miR-107 and miR-195) all include a 7-nt common sequence: AGCAGCA (Figure 1). Our study is not able to assess different developmental stages where alterations are known to occur in terms of miR-15/107 family member expression. For example, miR-15 and miR-16 expression correlates to particular stages in erythropoiesis [22,23]. Assessing archival human brains that had been formalin-fixed and paraffin-embedded, we found that miR-16 expression is highly expressed during early human brain development [24].

The current study confirms some of the prior observations with regard to miR-15/107 expression profiling experiments: gene expression among miR-15/107 group members

Table 2 Relative expression of miRNAs in primary rat neuronal and microglial cultures

miRNA	Microglia		Neurons	
	Fold change	*P* value	Fold change	*P* value
hsa-let-7a	0.781	0.023	1.880	0.028
hsa-miR-103	1.450	0.062	3.270	0.029
hsa-miR-107	0.840	0.383	4.020	0.005
hsa-miR-124a	2.900	0.137	8541.360	0.001
hsa-miR-143	0.036	0.028	0.008	0.003
hsa-miR-15a	1.240	0.428	2.050	0.021
hsa-miR-15b	0.441	0.112	1.140	0.333
hsa-miR-16	1.380	0.175	2.240	0.006
hsa-miR-195	0.208	0.009	1.490	0.183
hsa-miR-20a	1.150	0.244	5.320	0.001
hsa-miR-23a	1.710	0.001	0.114	0.000
hsa-miR-27a	1.320	0.137	0.123	0.002
hsa-miR-27b	1.370	0.310	0.599	0.097
hsa-miR-29a	0.926	0.298	0.091	0.003
hsa-miR-29b	1.460	0.009	0.093	0.014
hsa-miR-29c	1.270	0.110	0.311	0.134
hsa-miR-30d	4.910	0.006	3.130	0.009
hsa-miR-320	0.379	0.001	1.430	0.101
hsa-miR-424	0.746	0.428	0.676	0.333
hsa-miR-497	0.071	0.023	2.670	0.000
hsa-miR-503	1.500	0.298	0.971	0.953

Note: Expression of miRNAs in cultured rat neurons or microglial cells is normalized to that in astrocyte preparation and presented as fold changes. Expression that is significantly higher or low in neurons or microglial cells is highlighted in red and green, respectively ($P < 0.05$). Members of miR-15/107 family are highlighted in blue.

tends not to be purely specific to particular tissues or cell types. Furthermore, despite the caveat that Ct values of qPCR analyses cannot be confidently compared across transcripts, in humans the highest-expressing miRNAs tend to be miR-15a, miR-15b, miR-16, miR-103 and miR-107. The more recently evolved miRNAs (miR-424 and the primate-specific miR-646) show relatively low expression but the mammal-specific miR-195/miR-497 (physically close to each other on Chromosome 17) have moderate expression levels.

There has been inconsistency among prior studies in terms of miR-15/107 gene group member expression profiling in mammals, possibly due to technical issues. A subset of these miRNA genes has been detected in mammalian tissues including heart, skeletal muscle, brain, lung, liver, kidney, spleen and placenta [25–31]. There may be similar expression profiles among some group members across human tissues (miR-15, miR-16 and miR-195) [27], although some but not all studies have indicated that miR-15/miR-16 expression is relatively high in hematopoietic cells including T lymphocytes [25,26,28,32–35].

We found evidence to support miR-107 expression tropism for the human brain, and also rat neurons versus other cell types. Prior studies have provided mixed perspectives on whether miR-107 levels are highest in brain [27–29,31,35–37]. The complexity of this situation is illustrated in a study of embryos from different species using miRNA *in situ* hybridization, finding that miR-107 is essentially brain-specific in the Japanese killifish, highly expressed in almost all tissues in chicken, but neither pattern is observed in mouse [38].

Assessment of pri-miRNA levels using qPCR provided a new perspective on the rather poor correlation between levels of mature miRNAs and their precursors. This basic observation had been made previously by others in the context of miR-103 and miR-107 precursors [37] in mice tissues. We also note that miR-103a-2 appears much more highly expressed than miR-103a-1 in all human tissues, suggesting that this gene is the more transcriptionally active source of mature human miR-103. The discordant correlations of miRNA and the precursor were also reported for other miRNAs [39]. These observations confirm the importance and regulatory relevance of the processing steps of miRNA biogenesis. In contrast to the generally discordant correlation between levels of detected precursor and mature miRNA, expression of miR-124 seems to be highly correlated between mature and precursor – the brain-specific expression of miR-124a [40] has been demonstrated previously [39,40].

One key point that is strongly underscored by our data is that in a paralogous miRNA family, the cumulative impact of those miRNAs must be addressed rather than only focusing on one single gene family member. In other words, since miR-15/107 miRNAs have highly overlapping targets [7,16,41], and multiple members of the gene family are transcribed at constitutively high levels, any therapeutic or diagnostic method based on one family member must also take into account the biological activities of other family members. We conclude that this added level of complexity, related to multiple paralogs with overlapping targets, is particularly important in miR-15/107 family of miRNAs.

TaqMan assays developed for miRNA detection and validation proved to be sensitive and easy to use [42]. The more recent TaqMan PCR-array platform is a reproducible methodology in miRNA profiling with a broad dynamic range. In this study, we used TaqMan's Low Density Arrays (TLDA) which is a medium-throughput method of real-time RT-PCR array. This system offers flexibility to tailor the probe groups, such as the one we employed here for miR-15/107 family profiling.

There is a persistent challenge of normalization in miRNA expression studies across cell types and tissues [43–47]. We hypothesize it may not be possible to find a "one size fits all" normalization method. Although the custom array card included internal controls (U6 and RNU66 for mature miRNAs; beta-actin and GAPDH for the precursors) in the panel, we could not rely on these controls to normalize the data because of the substantial variability of these genes expressed in tissues and cells (Tables S3, S4 and S5). In mature miRNA panels, the standard deviations for U6 and RNU66 are 2.1 and 2.5 Ct, respectively (equivalent to 4.3- and 5.7-fold difference); and in the miRNA precursor panel, the standard deviations for beta-actin and GAPDH

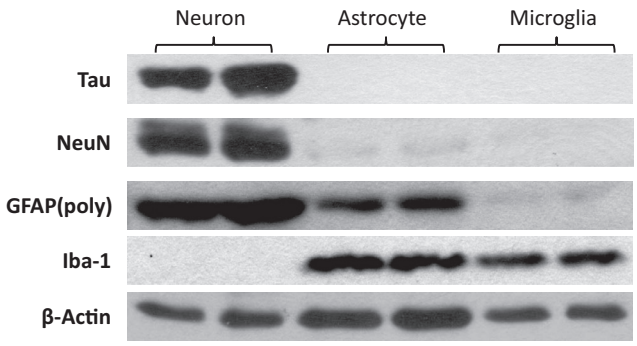

Figure 4 Western blot verification of different primary rat brain cell cultures

Cell lysates of primary rat cell preparations enriched for cortical neurons, astrocytes or microglia cells were separated on SDS–PAGE and transferred to nitrocellulose membrane. Western blot analysis was carried out using cell marker antibodies: anti-NeuN monoclonal antibody (neuronal marker), anti-MAP-Tau antibody (neuronal marker), anti-GFAP polyclonal antibody (astrocyte marker) and anti-Iba-1-polyclonal antibody (microglia marker).

are 3.4 and 4.0 Ct, respectively (equivalent to 10.6- and 16-fold difference). The global mean normalization method [48] used in our dataset appeared to represent a best fit for the dataset after further validation on selected individual miRNAs. When normalizing TLDA data, one should take into consideration the careful choices of specific internal controls for normalization to avoid technical bias.

Materials and methods

High-throughput method for miR-15/107 target identification

Experiments were performed as described in detail previously [49,50]. Briefly, H4 cells (American Type Culture Collection, Manassas, VA) were cultured under the vendor's recommended conditions. Cells were transfected with 25 nM of exogenous RNA duplexes (Ambion, Austin, TX), using RNAiMAX (Invitrogen, Carlsbad, CA) according to manufacturer's instructions, and harvested 48 h after transfection. Total RNA was isolated, reversely transcribed to cDNA for

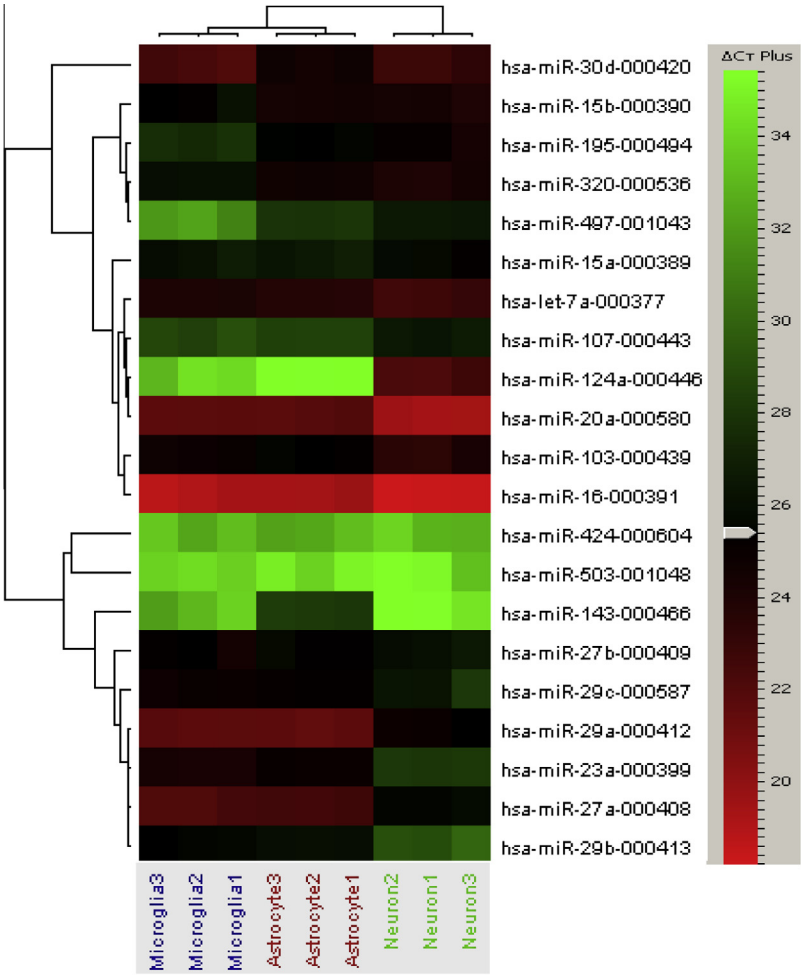

Figure 5 Hierarchical clustering of miRNA expression in primary rat cells

Ct values were normalized using the global mean method. The average linkage of the clustered group was calculated using the Pearson's correlation method. The heat map demonstrated the characteristic expression patterns of miR-15/107 family miRNAs. Other miRNAs, such as miR-124a, are almost exclusively expressed in neuronal cells. In contrast, some miRNAs (miR-23a, miR-27a, miR-29a, miR-29b and miR-143) are enriched in cultured glial preparations. Same cell types were marked in the same colors.

expression profiling using Affymetrix 1.0 ST Gene microarrays according to manufacturer's instructions. A total of 21,898 annotated genes were profiled. Genes were evaluated and determined to be targets when mRNA expression levels were lower in relative to the negative control miRNA transfections ($N = 3$ biological replicates for each transfection, $P < 0.01$ by Student's t-test).

Human tissues

All sample collection and experimental procedures involving human subjects were in compliant with the University of Kentucky Institutional Review board (IRB) protocols. Eleven human tissues from three autopsied individuals, coded as Case2, Case5 and Case7, with relatively intact RNA, were used in this work. Information on the autopsied individuals is shown in Table S2. Tissues included the cerebral cortex (left) (CECTX-L), frontal cortex (left) (FCTX-L), primary visual cortex (left) (PVCTX-L), thymus (THY), heart (HRT), lung (left) (LNG-L), liver (LVR), kidney (left) (KID-L), spleen (SPL), stomach (STO) and skeletal muscle (SKMSCL). The heart tissue of Case5 was not available. The samples from each tissue type were obtained with fresh scalpels, snap-frozen in liquid nitrogen and stored at −80 °C.

Primary rat cortex neuron, astrocyte and microglia culture

Animal handling was conducted following the University's Institutional Animal Care and Use Committee (IACUC) protocols. Primary cortical neuronal culture, primary astrocyte and microglial cultures (all are cell-type enriched, rather than pure preparations) were generated from Sprague–Dawley rat pups at E18 as described in [51,52]. All primary cell cultures were maintained at 37 °C in humidified, CO_2 (5%) incubator.

RNA isolation

Total RNA was extracted from human tissues or primary rat neuron, astrocyte and microglia cells using TRIZOL LS reagent (Life Technologies, USA) following the modified procedure described previously [18,47].

Western blot analysis

Conventional SDS–PAGE and Western blot analysis was performed as described previously [11]. Antibodies used in this work include anti-NeuN monoclonal antibody (neuronal marker, Chemicon, MAB377), anti-MAP-Tau antibody

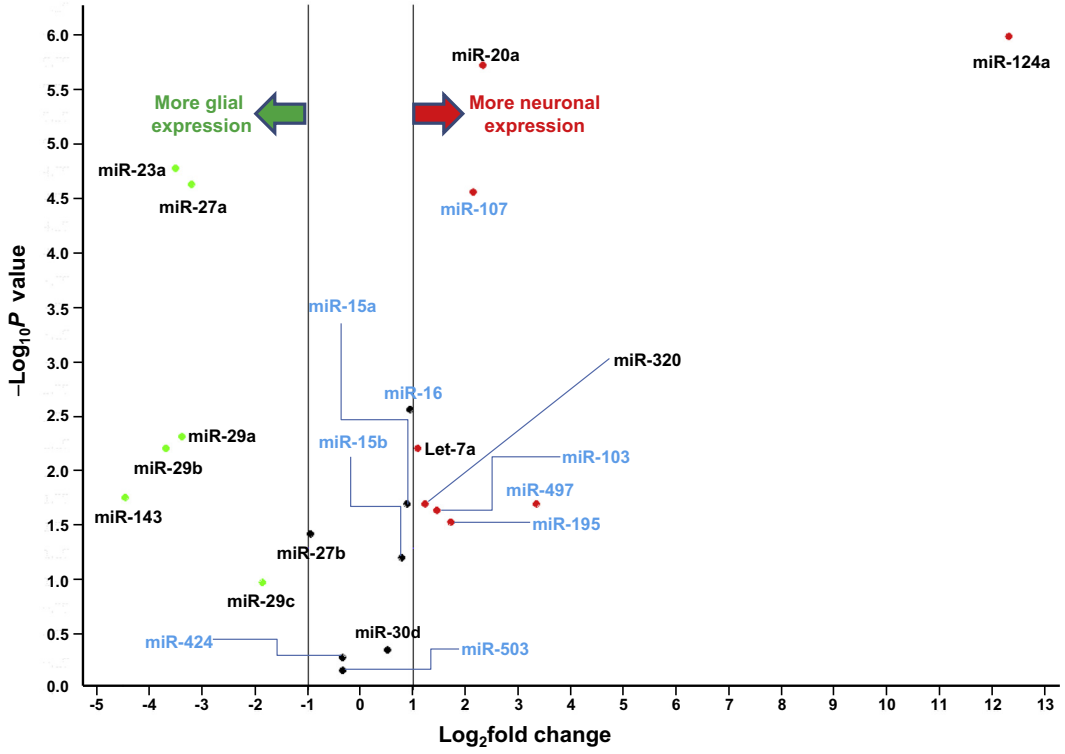

Figure 6 Volcano plot of expression of tested miRNAs in primary rat cells

This plot helps to visualize the degree of enrichment for individual miRNAs in neuronal *vs* non-neuronal (astrocyte and microglia) cell preparations. The threshold was set at 2.0 and 0.05 for fold change and P value, respectively. Relative expression is presented as fold changes of miRNA expression in neuronal cells compared to non-neuronal cells. miRNAs with significantly-different expression are indicated in red (higher expression) and green (lower expression), respectively ($P < 0.05$). Members of miR-15/107 family are highlighted in blue.

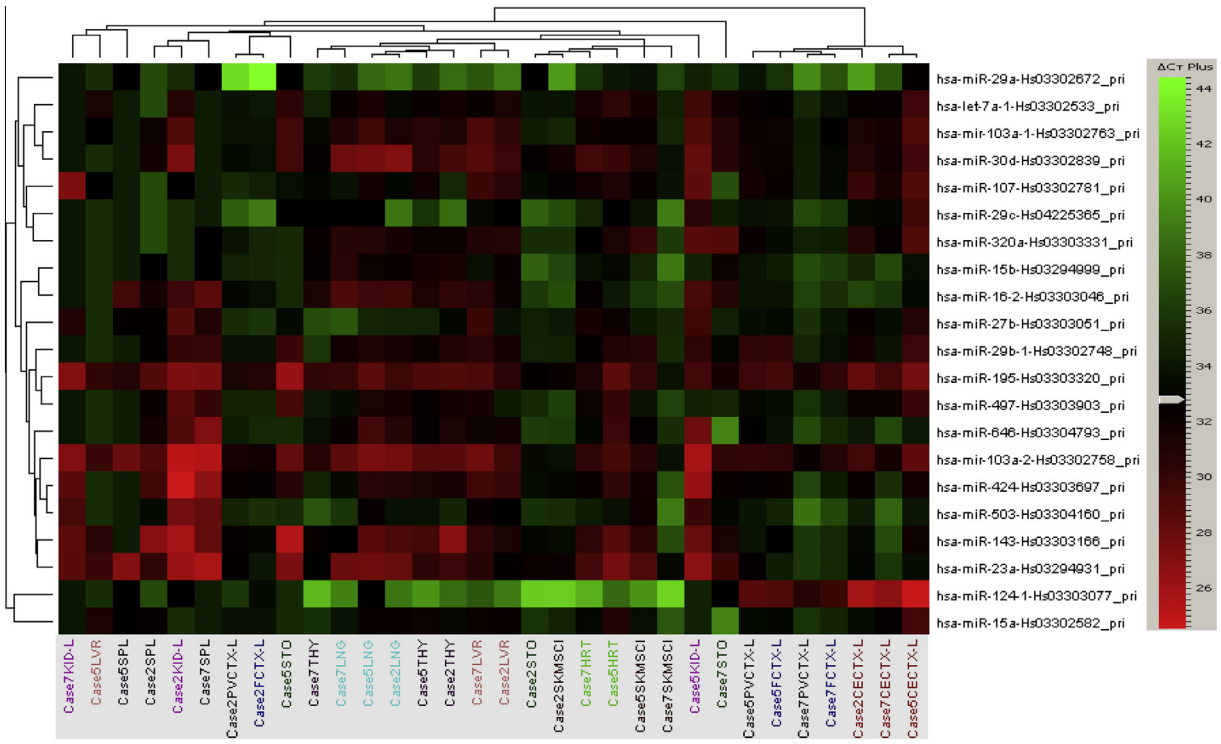

Figure 7 Hierarchical clustering of pri-miRNA expression

Ct values were normalized using global mean method in 11 human tissues. The average linkage of the clustered group was calculated using the Pearson's correlation method. Each tissue group was marked in the same color. CECTX-L, cerebral cortex (left); FCTX-L, frontal cortex (left); PVCTX-L, primary visual cortex (left); THY, thymus; HRT, heart; LNG-L, lung (left); LVR, liver; KID-L, kidney (left); SPL, spleen; STO, stomach; SKMSCL, skeletal muscle.

(neuronal marker, generously provided by Dr. Peter Davies), anti-GFAP polyclonal antibody (astrocyte marker, Sigma, G9269), anti-Iba-1 polyclonal antibody (microglia marker, Wako, 016-20001) and anti-beta-actin antibody (Rockland, 600401886).

miR-15/107 family profiling

We employed TaqMan Low-Density Array (TLDA) quantitative RT–PCR assays (Life Technologies) to study miRNA expression. Two panels of 24 assays each (Table S1) for mature miRNAs and their precursors including two endogenous controls (mammalian U6 and RNU66 for mature miRNA panel; beta-actin and GAPDH for the precursor panel), 10 members of miR-15/107 family and 12 other selected miRNAs, were custom prepared as an 8×24 array format (384 wells with 8 samples $\times$ 24 duplicate assays in each array card). Specific stem–loop primers for each mature miRNA were pooled and supplied by Life Technologies for reverse transcription (RT) reactions.

Total RNA (100 ng) was used for cDNA synthesis. For mature miRNA array, first-strand cDNA was synthesized using TaqMan® MicroRNA Reverse Transcription Kit (Life Technologies) with the pooled specific stem-loop primers. For miRNA precursor array, total RNA was first subjected to DNase treatment using Ambion® TURBO DNA-free™ kit (Life Technologies). The first-strand cDNA was synthesized using High Capacity RNA-to-cDNA Kit (Life Technologies). The resulting cDNAs served as templates for RT-qPCR profiling. PCR reaction mixtures for individual samples were transferred into the loading port on the customized TLDA cards (mature miRNA card, or precursor miRNA card), and loaded to each well by spinning the array card in a centrifuge according to the manufacturer's instructions. The card was then sealed and PCR was performed using ViiA™ 7 Real-Time PCR System (Life Technologies) with the following program: hold 2 min at 50 °C, followed by 10 min at 95 °C, then 40 cycles of 15 s at 95 °C and 1 min at 60 °C.

Data analyses

qPCR cycle threshold (Ct) raw data were processed with ViiA 7 RUO software (Life Technologies) excluding data that failed QC. miR-646 was removed from primary cell data set analysis, since mature miR-646 was not expressed in rat. We also removed the control RNU66 from the rat data set because it was amplified poorly (data not shown). As with the precursor panel, hsa-mir-92a-1 (precursor for miR-20a) was also excluded from analysis due to inefficient PCR amplification in all samples. Data from different array cards were then pooled for further analysis using DataAssist® software (Life Technologies). Averaged internal controls (U6 with or without RNU66 for mature miRNA cards, and beta-actin

Table 3 Relative expression of miRNA precursors in the human brain tissue

Precursor	Fold change	*P* value
hsa-let-7a-1-Hs03302533_pri	0.793	0.8655
hsa-mir-103a-1-Hs03302763_pri	0.714	0.835
hsa-mir-103a-2-Hs03302758_pri	0.318	0.0527
hsa-miR-107-Hs03302781_pri	1.200	0.9711
hsa-miR-124-1-Hs03303077_pri	585.700	0.0002
hsa-miR-143-Hs03303166_pri	0.072	0.0008
hsa-miR-15a-Hs03302582_pri	1.550	0.7661
hsa-miR-15b-Hs03294999_pri	0.424	0.1393
hsa-miR-16-2-Hs03303046_pri	0.181	0.0161
hsa-miR-195-Hs03303320_pri	0.917	0.9711
hsa-miR-23a-Hs03294931_pri	0.036	0.0000
hsa-miR-27b-Hs03303051_pri	0.741	0.8575
hsa-miR-29a-Hs03302672_pri	0.284	0.4629
hsa-miR-29b-1-Hs03302748_pri	0.971	0.9711
hsa-miR-29c-Hs04225365_pri	1.720	0.835
hsa-miR-30d-Hs03302839_pri	0.341	0.1045
hsa-miR-320a-Hs03303331_pri	0.980	0.9711
hsa-miR-424-Hs03303697_pri	0.228	0.0527
hsa-miR-497-Hs03303903_pri	0.781	0.8655
hsa-miR-503-Hs03304160_pri	0.210	0.0463
hsa-miR-646-Hs03304793_pri	0.223	0.0377

Note: Expression of miRNA precursors in human brain tissue is normalized to that in non-brain tissues and presented as fold change. Expression that is significantly higher or lower in brain is highlighted in red and green, respectively ($P < 0.05$). Members of miR-15/107 family are highlighted in blue.

and GAPDH for precursor miRNA cards) were used to calculate δCt (ΔCt) values of a given sample in relative to a selected reference sample. We found that endogenous genes are expressed differently across various tissues, making them inappropriate as internal controls, so instead of using the internal controls to normalize among various tissues, we used Global Mean normalization [48] to normalize the pooled dataset. miRNAs were considered undetectable with Ct value $\geqslant 35$ (mature miRNAs) or 40 (precursor miRNAs). Relative expression levels of mature miRNA or miRNA precursor were presented as fold change over a selected reference sample (*e.g.*, cerebral cortex).

Level of miRNA expression was evaluated using unpaired Student *t*-test and multiple testing using Benjamin-Hochberg false discovery rate (FDR) method was applied to correct the reported *P* values. $P < 0.05$ was considered as statistically significant.

Authors' contributions

WXW contributed to the design of the project, conducted the project and prepared the manuscript; PTN designed and oversaw the project, gathered tissue samples, supervised and contributed to the manuscript preparation; BSW contributed to tissue RNA isolation and Western blot analysis; CMN helped with primary rat brain cell culture preparation; RJD, CSM, JRB, NGV and JHN helped with autopsies, sample preparation and distribution, and data collection. All authors read and approved the final manuscript.

Competing interests

The authors have declared no completing interests.

Table 4 Expression correlation between mature and precursor miRNAs in human tissues

miRNA	Correlation coefficient (R^2)
hsa-let-7a	0.6229
hsa-miR-103-1	0.4655
hsa-miR-103-2	0.8357
hsa-miR-107	0.7086
hsa-miR-124a	0.9189
hsa-miR-143	0.1328
hsa-miR-15a	0.0569
hsa-miR-15b	0.0129
hsa-miR-16	0.1339
hsa-miR-195	0.3062
hsa-miR-23a	0.4538
hsa-miR-27a	0.5116
hsa-miR-27b	0.5003
hsa-miR-29a	0.3473
hsa-miR-29b	0.7067
hsa-miR-29c	0.5706
hsa-miR-30d	0.3161
hsa-miR-320	0.4067
hsa-miR-424	0.1683
hsa-miR-497	0.4361
hsa-miR-503	0.0273
hsa-miR-646	0.0023

Note: Relative expression levels of mature and precursor miRNAs in various human tissues were presented in Figure S1 and the correlation coefficient (R^2) were obtained by linear regression test. Members of miR-15/107 family are highlighted in bold.

Table 5 Relative expression of miR-103 precursors in different tissues

Tissue	Ct value		Fold change
	hsa-miR-103a-1	hsa-miR-103a-2	
Cerebral cortex	27.4	26.6	1.8
Frontal cortex	28.7	26.9	3.6
Heart	32.4	30.0	5.4
Kidney	35.9	31.2	24.8
Lung	31.8	28.9	7.2
Liver	34.3	31.7	5.8
Primary vision cortex	29.4	27.2	4.6
Skeletal muscle	32.3	30.9	2.7
Spleen	38.4	32.2	72.8
Stomach	32.5	31.5	2.1
Thymus	31.5	29.2	5.0

Note: Expression levels of two miR-103 precursors were presented as cycle threshold (Ct) or expressed as fold change. Fold change is calculated as $2^{-(Ct2-Ct1)}$, where Ct1 and Ct2 refers to the Ct value of has-miR-103a-1 and has-miR-103a-2, respectively.

Acknowledgements

This study was supported by the National Institutes of Health, USA (Grant Nos. AG042419, NS085830 and AG028 383).

Supplementary material

Supplementary data associated with this article can be found, in the online version, at http://dx.doi.org/10.1016/j.gpb.2013.10.003.

References

[1] Lewis BP, Burge CB, Bartel DP. Conserved seed pairing, often flanked by adenosines, indicates that thousands of human genes are microRNA targets. Cell 2005;120:15–20.
[2] Friedman RC, Farh KK, Burge CB, Bartel DP. Most mammalian mRNAs are conserved targets of microRNAs. Genome Res 2009;19:92–105.
[3] Miranda KC, Huynh T, Tay Y, Ang YS, Tam WL, Thomson AM, et al. A pattern-based method for the identification of microRNA binding sites and their corresponding heteroduplexes. Cell 2006;126:1203–17.
[4] Liu X, Fortin K, Mourelatos Z. MicroRNAs: biogenesis and molecular functions. Brain Pathol 2008;18:113–21.
[5] Bartel DP. MicroRNAs: target recognition and regulatory functions. Cell 2009;136:215–33.
[6] Mourelatos Z. Small RNAs: the seeds of silence. Nature 2008;455:44–5.
[7] Finnerty JR, Wang WX, Hebert SS, Wilfred BR, Mao G, Nelson PT. The miR-15/107 group of microRNA genes: evolutionary biology, cellular functions, and roles in human diseases. J Mol Biol 2010;402:491–509.
[8] Zhu W, Zhu D, Lu S, Wang T, Wang J, Jiang B, et al. miR-497 modulates multidrug resistance of human cancer cell lines by targeting BCL2. Med Oncol 2012;29:384–91.
[9] Moncini S, Salvi A, Zuccotti P, Viero G, Quattrone A, Barlati S, et al. The role of miR-103 and miR-107 in regulation of CDK5R1 expression and in cellular migration. PLoS One 2011;6:e20038.
[10] Nelson PT, Wang WX, Mao G, Wilfred BR, Xie K, Jennings MH, et al. Specific sequence determinants of miR-15/107 microRNA gene group targets. Nucleic Acids Res 2011;39:8163–72.
[11] Wang WX, Kyprianou N, Wang X, Nelson PT. Dysregulation of the mitogen granulin in human cancer through the miR-15/107 microRNA gene group. Cancer Res 2010;70:9137–42.
[12] Hebert SS, Wang WX, Zhu Q, Nelson PT. A study of small RNAs from cerebral neocortex of pathology-verified Alzheimer's disease, dementia with lewy bodies, hippocampal sclerosis, frontotemporal lobar dementia, and non-demented human controls. J Alzheimers Dis 2013;35:335–48.
[13] Wilfred BR, Wang WX, Nelson PT. Energizing miRNA research: a review of the role of miRNAs in lipid metabolism, with a prediction that miR-103/107 regulates human metabolic pathways. Mol Genet Metab 2007;91:209–17.
[14] Kriegel AJ, Liu Y, Fang Y, Ding X, Liang M. The miR-29 family: genomics, cell biology, and relevance to renal and cardiovascular injury. Physiol Genomics 2012;44:237–44.
[15] Mott JL, Kurita S, Cazanave SC, Bronk SF, Werneburg NW, Fernandez-Zapico ME. Transcriptional suppression of mir-29b-1/mir-29a promoter by c-Myc, hedgehog, and NF-kappaB. J Cell Biochem 2010;110:1155–64.
[16] Wang WX, Wilfred BR, Xie K, Jennings MH, Hu YH, Stromberg AJ, et al. Individual microRNAs (miRNAs) display distinct mRNA targeting "rules". RNA Biol 2010;7:373–80.
[17] Git A, Dvinge H, Salmon-Divon M, Osborne M, Kutter C, Hadfield J, et al. Systematic comparison of microarray profiling, real-time PCR, and next-generation sequencing technologies for measuring differential microRNA expression. RNA 2010;16:991–1006.
[18] Wang WX, Wilfred BR, Baldwin DA, Isett RB, Ren N, Stromberg A, et al. Focus on RNA isolation: obtaining RNA

for microRNA (miRNA) expression profiling analyses of neural tissue. Biochim Biophys Acta 2008;1779:749–57.
[19] Chen Y, Gelfond JA, McManus LM, Shireman PK. Reproducibility of quantitative RT-PCR array in miRNA expression profiling and comparison with microarray analysis. BMC Genomics 2009;10:407.
[20] Ach RA, Wang H, Curry B. Measuring microRNAs: comparisons of microarray and quantitative PCR measurements, and of different total RNA prep methods. BMC Biotechnol 2008;8:69.
[21] Willenbrock H, Salomon J, Sokilde R, Barken KB, Hansen TN, Nielsen FC, et al. Quantitative miRNA expression analysis: comparing microarrays with next-generation sequencing. RNA 2009;15:2028–34.
[22] Bruchova H, Yoon D, Agarwal AM, Mendell J, Prchal JT. Regulated expression of microRNAs in normal and polycythemia vera erythropoiesis. Exp Hematol 2007;35:1657–67.
[23] Choong ML, Yang HH, McNiece I. MicroRNA expression profiling during human cord blood-derived CD34 cell erythropoiesis. Exp Hematol 2007;35:551–64.
[24] Nelson PT, Baldwin DA, Kloosterman WP, Kauppinen S, Plasterk RH, Mourelatos Z. RAKE and LNA-ISH reveal microRNA expression and localization in archival human brain. RNA 2006;12:187–91.
[25] Bargaje R, Hariharan M, Scaria V, Pillai B. Consensus miRNA expression profiles derived from interplatform normalization of microarray data. RNA 2010;16:16–25.
[26] Shingara J, Keiger K, Shelton J, Laosinchai-Wolf W, Powers P, Conrad R, et al. An optimized isolation and labeling platform for accurate microRNA expression profiling. RNA 2005;11:1461–70.
[27] Baskerville S, Bartel DP. Microarray profiling of microRNAs reveals frequent coexpression with neighboring miRNAs and host genes. RNA 2005;11:241–7.
[28] Sempere LF, Freemantle S, Pitha-Rowe I, Moss E, Dmitrovsky E, Ambros V. Expression profiling of mammalian microRNAs uncovers a subset of brain-expressed microRNAs with possible roles in murine and human neuronal differentiation. Genome Biol 2004;5:R13.
[29] Babak T, Zhang W, Morris Q, Blencowe BJ, Hughes TR. Probing microRNAs with microarrays: tissue specificity and functional inference. RNA 2004;10:1813–9.
[30] Liu CG, Spizzo R, Calin GA, Croce CM. Expression profiling of microRNA using oligo DNA arrays. Methods 2008;44:22–30.
[31] Peltier HJ, Latham GJ. Normalization of microRNA expression levels in quantitative RT-PCR assays: identification of suitable reference RNA targets in normal and cancerous human solid tissues. RNA 2008;14:844–52.
[32] Wu H, Neilson JR, Kumar P, Manocha M, Shankar P, Sharp PA, et al. miRNA profiling of naive, effector and memory CD8 T cells. PLoS One 2007;2:e1020.
[33] Merkerova M, Belickova M, Bruchova H. Differential expression of microRNAs in hematopoietic cell lineages. Eur J Haematol 2008;81:304–10.
[34] Liu CG, Calin GA, Meloon B, Gamliel N, Sevignani C, Ferracin M, et al. An oligonucleotide microchip for genome-wide micr-oRNA profiling in human and mouse tissues. Proc Natl Acad Sci U S A 2004;101:9740–4.
[35] Wang Y, Weng T, Gou D, Chen Z, Chintagari NR, Liu L. Identification of rat lung-specific microRNAs by micoRNA microarray: valuable discoveries for the facilitation of lung research. BMC Genomics 2007;8:29.
[36] Soares AR, Pereira PM, Santos B, Egas C, Gomes AC, Arrais J, et al. Parallel DNA pyrosequencing unveils new zebrafish microRNAs. BMC Genomics 2009;10:195.
[37] Polster BJ, Westaway SK, Nguyen TM, Yoon MY, Hayflick SJ. Discordant expression of miR-103/7 and pantothenate kinase host genes in mouse. Mol Genet Metab 2010;101:292–5.
[38] Ason B, Darnell DK, Wittbrodt B, Berezikov E, Kloosterman WP, Wittbrodt J, et al. Differences in vertebrate microRNA expression. Proc Natl Acad Sci U S A 2006;103:14385–9.
[39] Lee EJ, Baek M, Gusev Y, Brackett DJ, Nuovo GJ, Schmittgen TD. Systematic evaluation of microRNA processing patterns in tissues, cell lines, and tumors. RNA 2008;14:35–42.
[40] Lagos-Quintana M, Rauhut R, Yalcin A, Meyer J, Lendeckel W, Tuschl T. Identification of tissue-specific microRNAs from mouse. Curr Biol 2002;12:735–9.
[41] Linsley PS, Schelter J, Burchard J, Kibukawa M, Martin MM, Bartz SR, et al. Transcripts targeted by the microRNA-16 family cooperatively regulate cell cycle progression. Mol Cell Biol 2007;27:2240–52.
[42] Schmittgen TD, Lee EJ, Jiang J, Sarkar A, Yang L, Elton TS, et al. Real-time PCR quantification of precursor and mature microRNA. Methods 2008;44:31–8.
[43] Wylie D, Shelton J, Choudhary A, Adai AT. A novel mean-centering method for normalizing microRNA expression from high-throughput RT-qPCR data. BMC Res Notes 2011;4:555.
[44] Lin YL, Lai ZX. Evaluation of suitable reference genes for normalization of microRNA expression by real-time reverse transcription PCR analysis during longan somatic embryogenesis. Plant Physiol Biochem 2013;66:20–5.
[45] Lim QE, Zhou L, Ho YK, Wan G, Too HP. SnoU6 and 5S RNAs are not reliable miRNA reference genes in neuronal differentiation. Neuroscience 2011;199:32–43.
[46] Brattelid T, Aarnes EK, Helgeland E, Guvaag S, Eichele H, Jonassen AK. Normalization strategy is critical for the outcome of miRNA expression analyses in the rat heart. Physiol Genomics 2011;43:604–10.
[47] Nelson PT, Wang WX, Wilfred BR, Tang G. Technical variables in high-throughput miRNA expression profiling: much work remains to be done. Biochim Biophys Acta 2008;1779:758–65.
[48] Mestdagh P, Van Vlierberghe P, De Weer A, Muth D, Westermann F, Speleman F, et al. A novel and universal method for microRNA RT-qPCR data normalization. Genome Biol 2009;10:R64.
[49] Wang WX, Wilfred BR, Hu Y, Stromberg AJ, Nelson PT. Anti-Argonaute RIP-Chip shows that miRNA transfections alter global patterns of mRNA recruitment to microribonucleoprotein complexes. RNA 2010;16:394–404.
[50] Wang WX, Wilfred BR, Madathil SK, Tang G, Hu Y, Dimayuga J, et al. MiR-107 regulates granulin/progranulin with implications for traumatic brain injury and neurodegenerative disease. Am J Pathol 2010;177:334–45.
[51] Norris CM, Blalock EM, Thibault O, Brewer LD, Clodfelter GV, Porter NM, et al. Electrophysiological mechanisms of delayed excitotoxicity: positive feedback loop between NMDA receptor current and depolarization-mediated glutamate release. J Neurophysiol 2006;96:2488–500.
[52] Sama MA, Mathis DM, Furman JL, Abdul HM, Artiushin IA, Kraner SD, et al. Interleukin-1beta-dependent signaling between astrocytes and neurons depends critically on astrocytic calcineurin/NFAT activity. J Biol Chem 2008;283:21953–64.